

Combining experimental and modelling approach to study the sources of reactive species induced in water by the COST RF plasma jet

Y. Gorbanev, C. C. W. Verlackt, S. Tinck, E. Tuenter, K. Foubert, P. Cos, A. Bogaerts

ELECTRONIC SUPPORTING INFORMATION

Contents

Fig. S1. Calibration curves obtained in the EPR experiments and UV experiments.....	p.2
Fig. S2. Time resolved formation of the PBN-H radical adduct in aqueous solutions of PBN exposed to COST RF jet.....	p.2
Fig. S3. Schematic representation of the geometry used in the fluid dynamics model.....	p.3
Table S1. Amount of H ₂ O in the D ₂ O samples for different conditions as determined by ¹ H-NMR.....	p.3
Table S2. The calculated concentration of reactive species in the plasma effluent, obtained from the 0D chemical kinetics model.....	p.4
Fig. S4. Velocity profiles of the gas in the effluent calculated by the 3D fluid dynamics model for the system with a 10 mm gap, with and without side flow.....	p.4
Fig. S5. Typical EPR spectra obtained in the experiments with DMPO solution in H ₂ O exposed to the COST RF plasma jet.....	p.4
Fig. S6. The effect of H ₂ O vapour content in the feed and the side flow gas on the formation of the DMPO-H radical adduct.....	p.5
Fig. S7. Typical EPR spectra obtained in the experiments with PBN solutions exposed to the COST RF plasma jet.....	p.5
Fig. S8. Experimental EPR spectra obtained by exposing solutions of PBN to the COST RF jet under various conditions.....	p.5
Table S3. Fraction of the PBN-H and PBN-D radical adducts formed in a liquid D ₂ O sample exposed to the COST RF plasma jet for different flushing times.....	p.6
Fig. S9. Concentration of the PBN radical adducts in the liquid exposed to the COST RF plasma jet as a function of the feed gas humidity (D ₂ O liquid, D ₂ O vapour).....	p.6
Fig. S10. Concentration of the PBN radical adducts in the liquid exposed to the COST RF plasma jet as a function of the side flow gas humidity (H ₂ O liquid, H ₂ O vapour).....	p.6
References.....	p.6

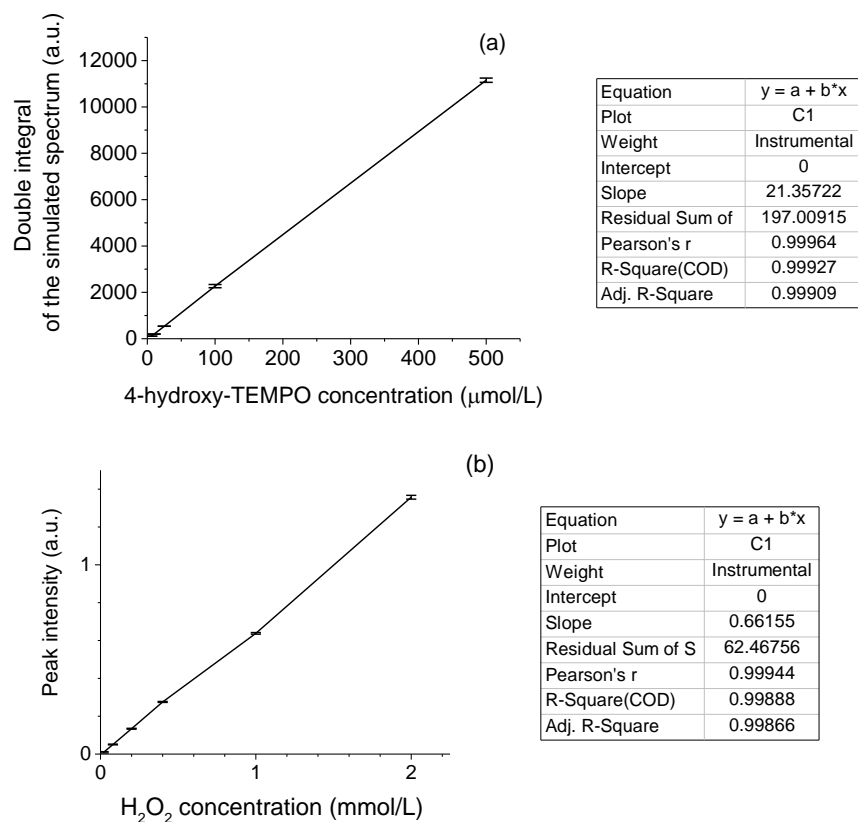


Figure S1. Calibration curves obtained in the EPR experiments with aqueous solutions of 4-hydroxy-TEMPO (a) and UV-Vis experiments with H_2O_2 (b).

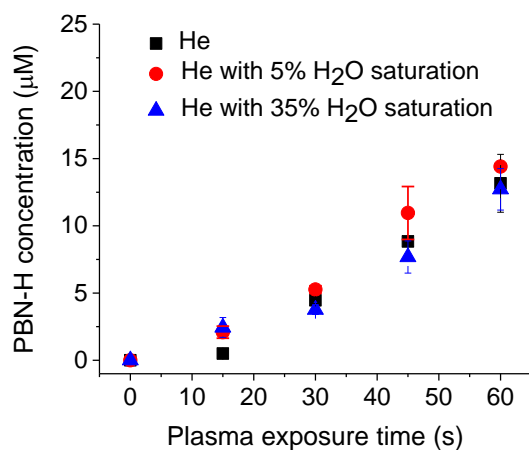


Figure S2. Time resolved formation of the PBN-H radical adduct in aqueous solutions of PBN (100 mM) exposed to a plasma with He, He with 5% H_2O saturation, and He with 35% H_2O saturation feed gas. The distance between the sample and the jet was 10 mm.

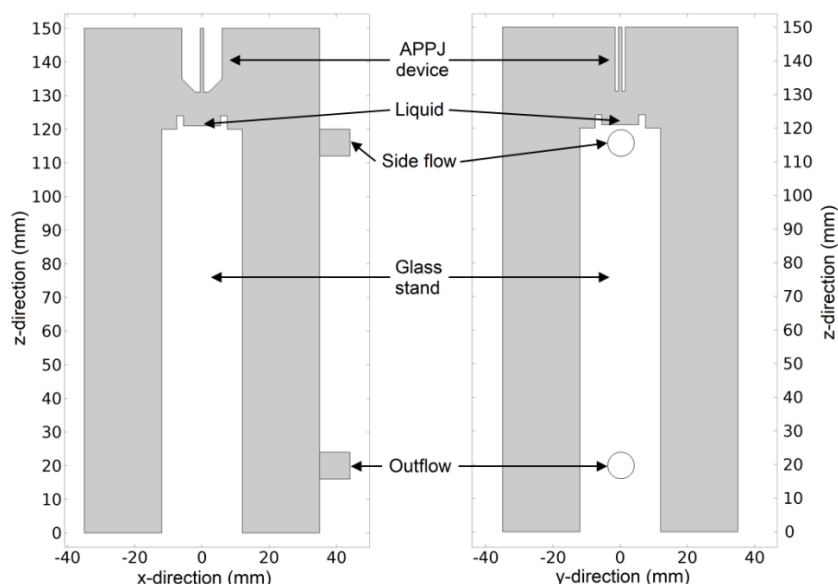


Figure S3. Schematic representation of the geometry used in the fluid dynamics model for the system with a gap of 10 mm. Left: XZ cross section at $Y=0$ mm; right: YZ cross section at $X=0$ mm. Only the grey area is considered in the calculation, *i.e.*, only the interior of the glass reactor (70 x 70 x 150 mm) and excluding the solid objects, like the COST plasma jet and the glass stand. The latter is modelled as a solid cylinder with a radius of 24 mm and a height of 120 mm. On this stand, the liquid sample is considered as a static surface (depth 1 mm, diameter 11 mm) between the borders of the well. From the top, the plasma jet is introduced based on the dimensions of the COST RF jet. In this jet, a 1 x 1 mm rectangular inlet is introduced. The position of the plasma jet nozzle was either 3 or 10 mm away from the liquid surface (see main paper). In the figure, a gap of 10 mm is shown. All walls are considered to be non-slip, meaning that the lateral velocity is 0 m/s. The pressure and temperature inside the glass reactor are set at a constant value of 1 atm and 294.5 K, respectively. The gas flowing in the reactor was He, with a density of 0.17 kg/m^3 and a dynamic viscosity of $2 \times 10^{-5} \text{ Pa}\cdot\text{s}$. The flow rate of the feed gas was set to 1 L/min, as in the experiments, reaching an average velocity of 26 m/s inside the plasma jet. Simulations were also performed with a side flow. This was implemented using a cylinder with a diameter of 8 mm positioned at a height of 112 mm in the glass reactor. The flow rate of the side flow was 2 L/min, corresponding to an average velocity of 1.3 m/s. The outlet is implemented using an identical cylindrical tube at a height of 16 mm from the bottom of the reactor. Water is introduced in the reactor either through the feed gas (plasma jet) or *via* the side flow. A diffusion coefficient of $0.282 \text{ cm}^2/\text{s}$ for water was used [1].

Table S1. Amount of H_2O in the D_2O samples for different conditions as determined by $^1\text{H-NMR}$.

Entry	Sample description	H_2O in the liquid D_2O after treatment ^[a] (mol%)
1	untreated commercial D_2O	0.1
2	D_2O with added sodium tosylate	0.1
3	D_2O with added 0.1 M PBN	0.1
4	D_2O after standing in reactor with no gas flow for 80 s	0.4

^[a]Determined by $^1\text{H-NMR}$ analysis with an external standard.

Table S2. The calculated concentration of reactive species in the plasma effluent, obtained from the 0D chemical kinetics model, at two distances from the end of the plasma jet, corresponding to the two different gaps between plasma jet and liquid in the experiments.

Entry	H ₂ O saturation of the feed gas (%)	Gap ^[a] (mm)	Reactive species concentration in the effluent (cm ⁻³)		
			H ₂ O ₂	OH	H
1	0	3	2.27×10^9	5.32×10^{11}	2.83×10^{11}
2	5		7.02×10^{13}	3.45×10^{13}	1.55×10^{14}
3	10		1.15×10^{14}	3.80×10^{13}	2.31×10^{14}
4	20		1.69×10^{14}	3.82×10^{13}	2.91×10^{14}
5	35		2.22×10^{14}	3.83×10^{13}	3.30×10^{14}
6	0	10	4.71×10^9	4.87×10^{11}	2.89×10^{11}
7	5		7.11×10^{13}	1.50×10^{13}	1.47×10^{14}
8	10		1.11×10^{14}	2.01×10^{13}	2.04×10^{14}
9	20		1.75×10^{14}	2.50×10^{13}	2.46×10^{14}
10	35		2.35×10^{14}	1.41×10^{13}	2.49×10^{14}

^[a]Distance from the end of the COST RF plasma jet.

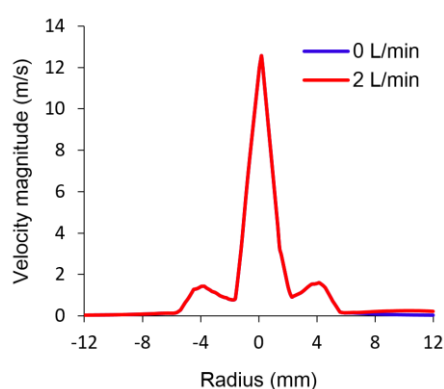


Figure S4. Velocity profiles of the gas in the effluent calculated by the 3D fluid dynamics model for the system with 10 mm gap, with and without side flow (red and blue, respectively). The velocity profile is determined at a height of 125 mm (6 mm below the nozzle). The central peak represents the effluent, while the two smaller peaks result from recirculation of the gas after the effluent comes in contact with the liquid (see Fig. 2 in the main text). An almost complete overlap between the two graphs is observed (with a small exception for the gas beyond the borders of the liquid vessel, *i.e.*, radius of 5.5 mm), meaning that a side flow of 2 L/min does not affect the plasma jet.

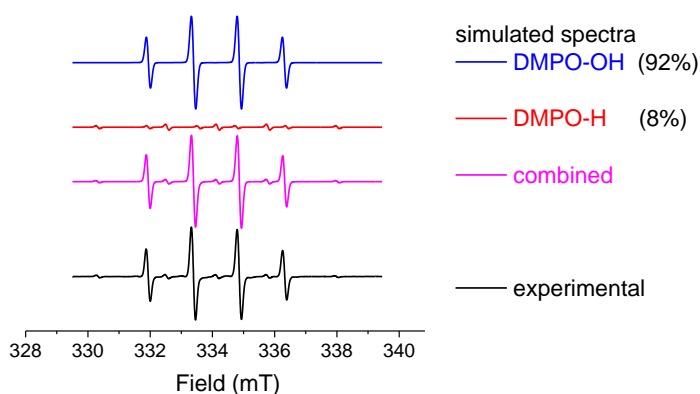


Figure S5. Typical EPR spectra (experimental and simulated) obtained in an experiment with DMPO solution in H₂O exposed to the COST RF plasma jet. Radical adducts: DMPO-OH ($a_N = 1.47$ mT, $a_H = 1.43$ mT); DMPO-H ($a_N = 1.62$ mT, $a_H = 2.23$ mT (x2)).

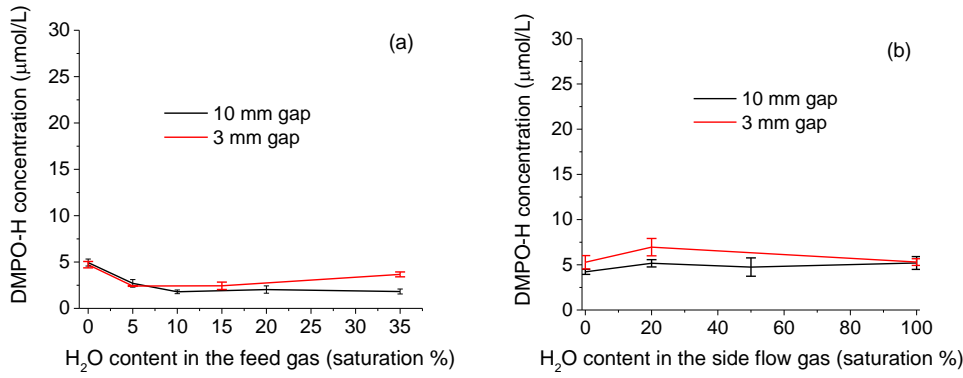


Figure S6. Effect of H_2O vapour content in the feed gas (a) and the side flow gas (b) on the formation of the DMPO-H radical adduct.

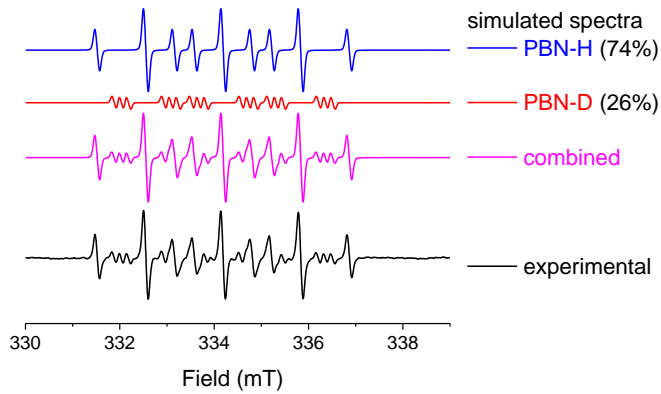


Figure S7. Typical EPR spectra (experimental and simulated) obtained in an experiment with PBN solutions exposed to the COST RF plasma jet. Radical adducts: PBN-H ($a_N = 1.64$ mT, $a_H = 1.03$ mT ($\times 2$)); PBN-D ($a_N = 1.64$ mT, $a_H = 1.05$ mT, $a_D = 0.15$ mT).

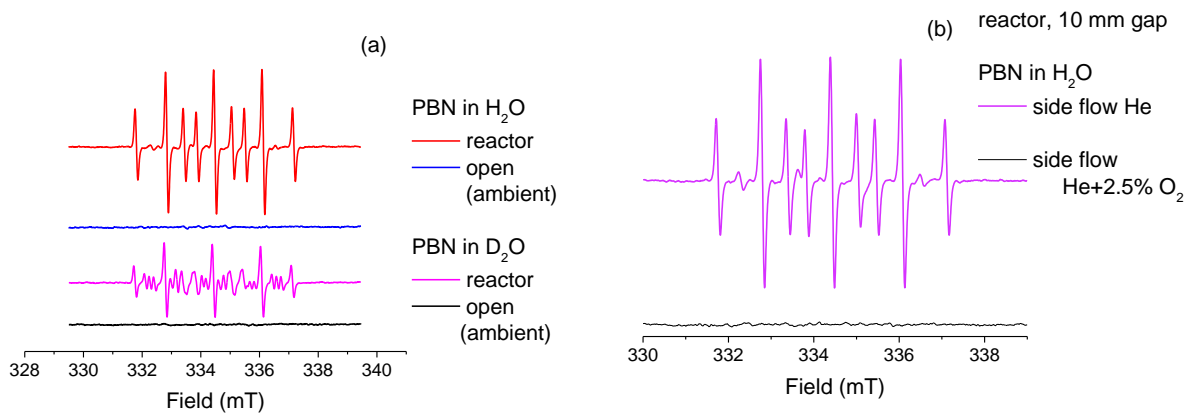


Figure S8. Experimental EPR spectra obtained by exposing solutions of PBN to the COST RF jet under various conditions. The presence of oxygen in the effluent (either from the ambient air (a) or introduced with the side flow of He (b)) results in the disappearance of the PBN-H/PBN-D radical adducts. The molecular oxygen used in this experiment was supplied by Praxair (99.5%).

Table S3. Fraction of the PBN-H and PBN-D radical adducts formed in a liquid D₂O sample exposed to the COST RF plasma jet for different flushing times. The plasma was ignited with He containing no added H₂O vapour.

Entry	Flushing time (min)	PBN-H ^[a] (%)	PBN-D ^[a] (%)
1	165	68	32
2	0.33	67	33
3	0.25	70	30

^[a]Determined by EPR analysis.

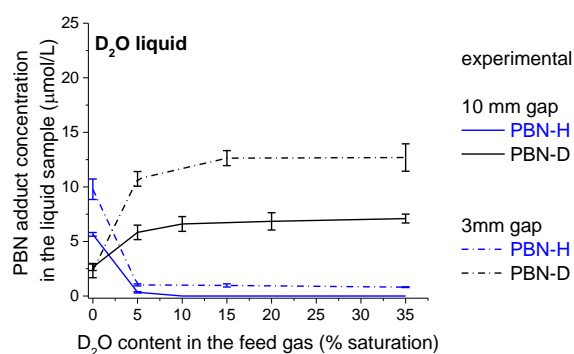


Figure S9. Concentration of the PBN radical adducts in the liquid exposed to the COST RF plasma jet as a function of the feed gas humidity. Plasma exposure conditions: D₂O liquid, D₂O feed gas. The concentrations of PBN-H and PBN-D were measured by EPR.

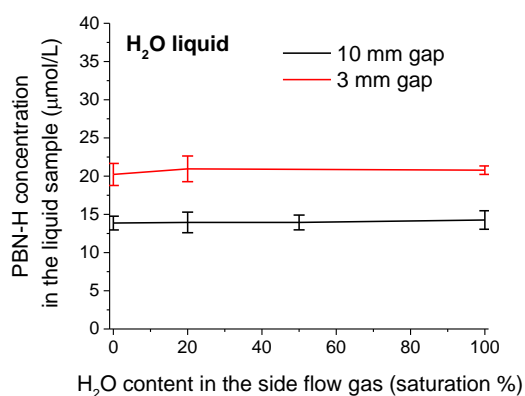


Figure S10. Concentration of the PBN radical adducts in the liquid exposed to the COST RF plasma jet as a function of the side flow gas humidity. Plasma exposure conditions: H₂O liquid, H₂O side flow gas. The concentration of PBN-H was measured by EPR.

References

[1] E. Cussler, *Diffusion: Mass Transfer in Fluid Systems (2nd ed.)*, 1997, Cambridge University Press, ISBN 0-521-45078-0.